Application of Experimental Design to Optimize the Synthesis of CdO Cauliflower-like Nanostructure Using Mechanochemical Method

A. Tadjarodi[*a], M. Imani[a], H. Kerdari[b]

[a]*Research Laboratory of Inorganic Materials Synthesis, Department of Chemistry, Iran University of Science and Technology, 16846-13114, Tehran, Iran*

[b]*Department of Chemistry, Saveh Branch, Islamic Azad University, Saveh, Iran*

*Corresponding author:
E-mail address:
tajarodi@iust.ac.ir
Phone: +98 (21) 77240516
Fax: +98 (21) 77491204

Abstract

Cauliflower-like nanostructure of cadmium oxide was synthesized by utilizing mechanochemical reaction followed calcination procedure for the first time. The design of experiment (DOE) by Taguchi method was used to study influence of the chosen factors and to consider optimum conditions of the experiments. The temperature of calcining, the duration of milling, the duration of calcining and reactants molar ratio (M/L) are four chosen factors for DOE. The value of band gap energy was calculated through UV-visible absorption spectroscopy and Tauc relation. Data analysis was performed using Minitab and Qualitek-4 statistical softwares. The optimum conditions for preparing cauliflower-like structure were predicted and also, influence of each factor was determined. The temperature and duration of calcining with the percentage contribution of 68.23 and 17.72%, respectively are the most effective factors at this design.

1. Introduction

Nowadays, semiconductor metal oxides in nanoscale have attracted a lot of attention because of their optical and electrical properties so that many investigations have developed in this field. Cadmium oxide, CdO, is a known n-type semiconductor with a direct band gap of 2.2-2.5 eV and an indirect band gap of 1.36-1.98 eV [1-4].

Meanwhile, there are reports that band gap of this material can change in a wide range from 1.1 to 3.3 eV due to mixing with appropriate materials [5-8]. Diversity in the optical band gap can be assigned to lattice's defects as a result of the Burstein-Moss effect [9]. In fact, optical and electrical properties of cadmium oxide nanostructures are related to the difference of band gaps in various structures.

Cadmium oxide nanostructures are applied in solar cells [10, 11], gas sensors [12-14], transparent electrodes [15-17] and photodiodes [18], catalysts and photocatalysts [19 -21] and optoelectronic devices [22, 23]. The numerous structures of cadmium oxide in nanoscale have been reported such as nanoparticles [1], nanowires [3, 4], thin films [10, 11], nanoneedles [17], nanotubes [24], nanorods [25], nanocrystals [26, 27].

There are several techniques to prepare these materials such as sonochemical [28, 29], microemulsion [1], hydrothermal/solvothermal method [30, 31] and mechanochemical process [32]. Mechanochemical procedure is the act of grinding associated to the chemical reaction in solid state. Mechanical alloying, the type of solid state reaction, was introduced by Benjamin in 1960s for the first time and then, it was developed as mechanochemical process to synthesize nanomaterials by McCormick [33]. In fact, this process is a simple and useful route so that can be a beneficial technique to prepare various nanomaterials in industry [33, 34]. Many efforts have been carried out to improve the reaction conditions and attain the efficient parameters. Design of experiment (DOE) is the powerful statistical technique to reach this aim. Taguchi method is a technique of DOE, which was introduced by Japanese researcher, Taguchi. This method is employed to optimize the synthesis conditions and improve the performance of process by reducing the number of experiments. Decrease the number of experiments is performed using orthogonal arrays and considering the factors and levels of each factor. The number of experiments is determined by formula of $L_n (X^Y)$, where n is number of rows in the array, Y is number of columns in the array and X is number of levels in the columns. In classical method by selecting four factors with three levels, $3^4=81$ experiments should be performed while these numbers are decreased to 9 experiments by using an orthogonal array of L_9 based on Taguchi method. In L_9, each row presents the levels of factors and each column is assigned to each factor. The Minitab and Qualitek-4 softwares are employed to analyze this data [35-38].

In this work, we synthesized cadmium oxide cauliflower-like nanostructure by utilizing mechanochemical reaction followed thermal processing. Then, we used Taguchi method to optimize the synthesis procedure of this structure using Minitab and Qualitek-4 statistical softwares. Due to choose four factors and three levels for each factor, the number of experiments reduced from 81 to 9. Since the band gap energy has an important role in the photocatalytic activity, this parameter was selected as response in DOE. Meanwhile, we investigated the relative influence of the chosen factors on the band gap energy. The structural and morphological characterization of the products at the all tests was performed using FT-IR, XRD, NMR, CHN, SEM and TEM.

2. Experimental

2.1 Materials

All of the chemical used in this work were purchased from Merck Co. and used without further purification.

2.2. Synthesis method

Cd(CH₃COO)₂.2H₂O and CH₃CONH₂ were used as starting materials to prepare the cauliflower-like nanostructures. The performance of the process was considered by four main factors with three levels of the each factor that is given in Table 1. By selecting factors and levels (Table 1) and using an orthogonal array of L9 (3^4) based on Taguchi method, were designed the number of 9 experiments according to Table 2. In order to perform these experiments, the mentioned reactants with organized molar ratio were milled each other by loading into a stainless steel 10 mL container including two small balls of 10 mm diameter in Mixer Mill apparatus (Retsch MM-400). The milling process was carried out in the solid state without any additives through the grinding container vibrations and the balls rotation at the fixed rate of 1800 rpm and designed periods of time. Then, the resultant precursors of grinding were calcinated at the temperatures and durations arranged in Table 2 to obtain the final products.

2.3. Characterization

The powder X-ray diffraction (XRD) measurements were carried out by a JEOL diffractometer with monochromatized Cu Kα radiation (λ =1.5418 Å). Fourier transform infrared (FT-IR) spectra were recorded on a Shimadzu-8400S spectrometer in the range of 400-4000 cm⁻¹ using KBr pellets. Scanning electron microscopy (SEM) images were taken on a Philips (XL-30) with gold coating. Optical absorption and transmission of the CdO nanostructures were evaluated in the range of 190-800 nm by using a UV–Vis spectrophotometer (Shimadzu-UV-2550-8030) with slit width of 5.0 nm and light source with wavelength of 360.0 nm at room temperature. ¹H NMR and ¹³C NMR spectra (500.13 MHz) were recorded using a Bruker AVANCE 500 spectrometer and remarked internally using the solvent reference relative to tetramethylsilane (TMS, δ 0). Chemical shifts (δ) are given in ppm. Elemental analysis was performed by utilizing a FOSS Heraeus CHN microanalyser. Transmission electron microscopy (TEM) images and electron diffraction patterns were taken on a Philips CM-200, FEG microscope.

3. Results and discussion

Nine experiments given in Table 2 were carried out and each of the resultant precursors and obtained products were characterized by FT-IR, ¹H NMR and ¹³C NMR spectroscopy, elemental analysis (CHN) and X-ray diffraction (XRD) pattern. The band gap energy was chosen as response of each test. Fig. 1 shows the FT-IR spectra after milling process (Fig. 1-a) and after heating treatment (Fig. 1-b). The observed peaks in Fig. 1-a are related to the organic section of the precursor.

Table 1. The selected factors and their levels.

Factor	Description	Level 1	Level 2	Level 3
A	Temprature of calcining (˚C)	350	450	550
B	Duration of milling (min)	30	60	90
C	Duration of calcining (h)	2	4	6
D	M/L ratio (molar)	3:2	3:4	3:6

The broad absorption band in the range of 3200 - 3350 cm^{-1} is assigned to the N-H anti-symmetrical and symmetrical stretching vibrations, which are in accordance to vibrations of the amine functional group. This broad band is a result of the overlapping O-H stretching band of H_2O molecule with the NH_2 vibrations. The appeared peaks in 1640 -1680 cm^{-1} are attributed to the stretching vibration of C=O with low frequency because of the resonance effect of the amide molecule. The bending vibration of N-H is observed at 1550 cm-1. The peaks at 1402, 1417 and 1346 cm^{-1} belong to the bending vibrations of CH_3 groups. Also, the observed weak bands at 1080, 1025, and 900 cm^{-1} may be assigned to overlapped C-N and C-O stretching vibrations. Probably, the weak peak at 673 cm^{-1} can be attributed to Cd-O stretching vibration formed in precursor molecule. The observed absorption bands of the organic parts in Fig. 1-a were removed after heating so that no peaks of organic molecules are observed in the spectrum of product

(Fig. 1-b) and only CdO phase remains. The data of FT-IR analysis is in a close agreement with each of the prepared samples given in Table 2.
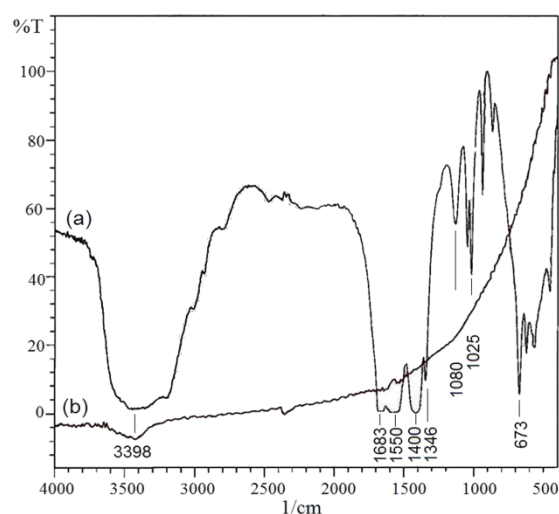
Fig. 1. FT-IR spectra of (a) the precursor and (b) the product.

XRD pattern (Fig. 2) demonstrates formation of the CdO phase as the product with lattice constant 4.695 Å and the space group $Fm\overline{3}m$. The diffraction peaks at 2θ values of 32.90˚, 38.20˚, 55.20˚, 65.80˚, and 69.20˚ matching with 111, 200, 220, 311, and 222 of cubic CdO (JCPDS- 05-0640) indicated the formation of CdO.

Table 2. Conditions of the tests.

	Temprature of calcining (˚C)	Duration of milling (min)	Duration of calcining (h)	M/L ratio (molar)
Test 1	350	30	2	3:2
Test 2	350	60	4	3:4
Test 3	350	90	6	3:6
Test 4	450	30	4	3:6
Test 5	450	60	6	3:2
Test 6	450	90	2	3:4
Test 7	550	30	6	3:4
Test 8	550	60	2	3:6
Test 9	550	90	4	3:2

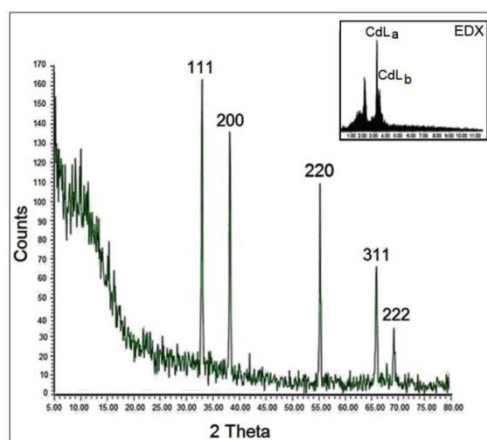No impurity was found in the sample. The EDX analysis and XRD pattern confirm CdO phase.

Fig. 2. XRD pattern and EDx analysis inserted to this pattern of the resultant product.

Elemental analysis (CHN) and NMR spectra were used to characterize the composition of the precursor as follows: Anal. Calcd. for: $(CdC_6H_{11}NO_5)$: C, 24.48: H, 3.79: N,4.8(%) . Found: C, 23.34: H, 3.9: N, 3.6 (%). Also, ^{1}H NMR and ^{13}C

NMR spectra of the obtained precursor have been shown in Fig. 3 and Fig. 4, respectively that confirm the mentioned structure. The shown peaks in figures were related to the protons and carbons of the intermediate molecule(precursor): ^{1}H NMR (MeOD, ppm) δ 6.93– 7.74 (NH$_2$), δ 6.001 (protons of the CH$_3$ group of the two acetate ligands) and δ 3.002 (protons of the CH$_3$ group of the acetamide ligand). ^{13}C NMR (MeOD, ppm) δ 21.9 (carbon of the methyl group of the acetate ligand) δ 22.1 (carbon of the methyl group of acetamide ligand) δ 177 (carbon of carbonyl group of the acetamide) and δ 181 (carbon of carbonyl group of the acetate ligand). Also, the assigned peak of the used solvent is observed at 49 ppm. By considering elemental analysis and NMR data, the molecular formula of precursor can be suggested as $Cd(CH_3CONH_2)(CH_3COO)_2$.

Fig. 5 shows the SEM images of obtained precursor. It is found that the grinding is led to the generation of this structure and then its growth is completed in furnace as it can be seen in Fig. 6. This figure shows SEM images of the obtained product after running each experiment that clearly depicts cauliflower-like

nanostructure of CdO. The high magnification of SEM images (Fig. 6 b-c) exhibited the cauliflower-like structure composed of rods.
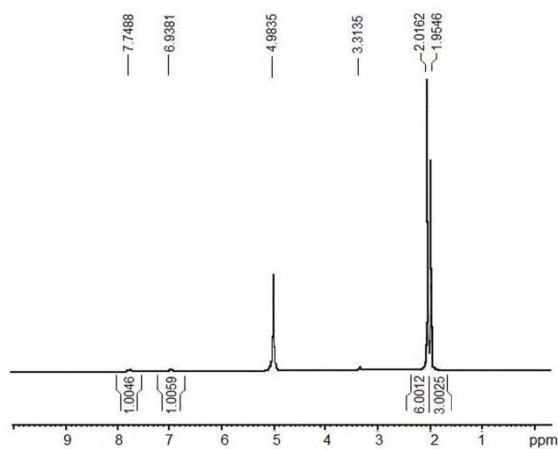

Fig. 3. ^{1}H NMR spectrum of the resulting precursor.
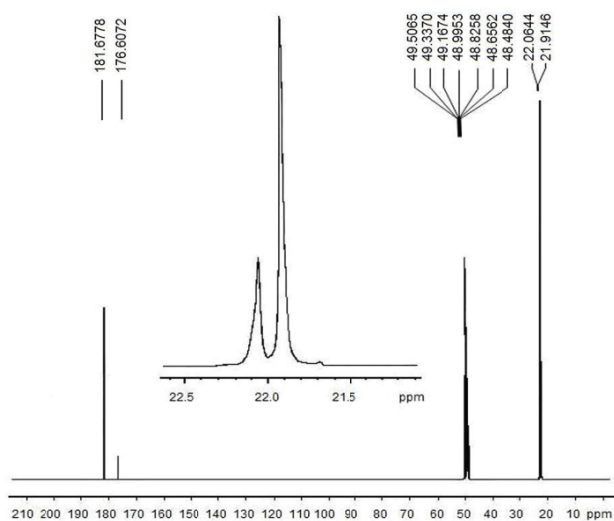

Fig. 4.^{13}C NMR spectrum of the obtained precursor.

Fig. 6-d with the higher magnification revealed that the average diameter of these rods is 59 nm. It was found that the running each experiment according to Table 2, is led to the formation of cauliflower-like structure.
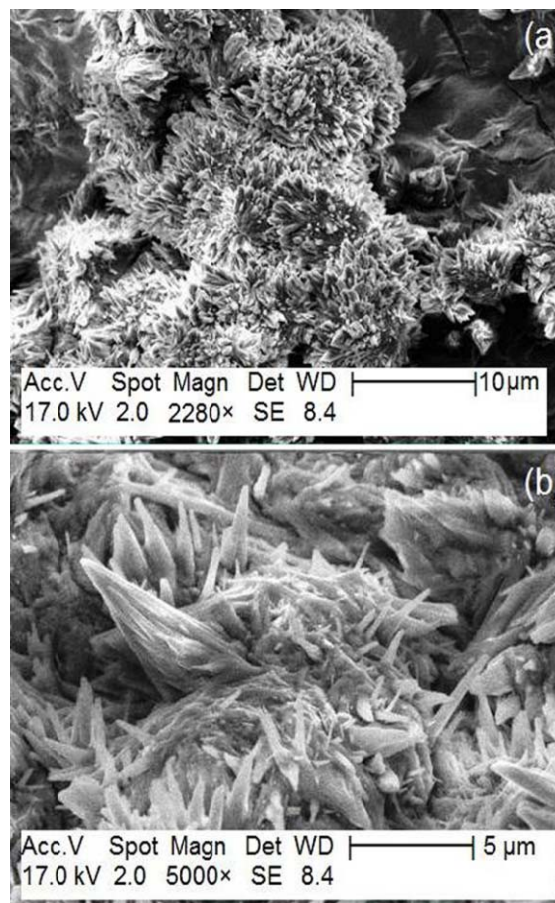

Fig. 5. SEM images of the precursor.

TEM images given in Fig.7 clearly show bundles of rods. In addition, there are tubes, which have combined with rods and formed final structure as cauliflower. It is possible that the assembly of particles with linear orientations is caused to growth of the rods and tubes. The coordination mode of the ligands to the cadmium ions at the intermediate molecule (precursor) can perform important role for the formation of the mentioned structure [39, 40]. Electron diffraction pattern inserted to TEM image in Fig 7-c reveals that the components of the cauliflower- like nanostructure have a single crystalline nature.
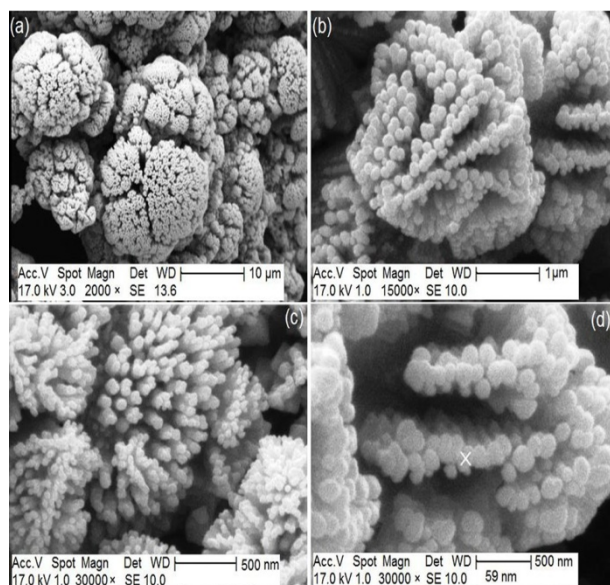
based on UV-Vis absorption spectrum given in Fig 8.

Fig. 6. SEM images of the product (a-d).

Table 3. The response and S/N ratio for each experiment.

Test #	Y (eV)	S/N ratio
1	2.08	6.361
2	2.19	6.808
3	2.01	6.059
4	2.04	6.192
5	1.90	5.575
6	2.07	6.319
7	1.85	5.343
8	1.92	5.666
9	1.83	5.249

After running each experiment, the direct band gap energy (*Eg*) as response of each test was obtained using Tauc relation and determining extrapolation point through plotting *(αhv)²* vs. *hv* (eV) (Fig 8)
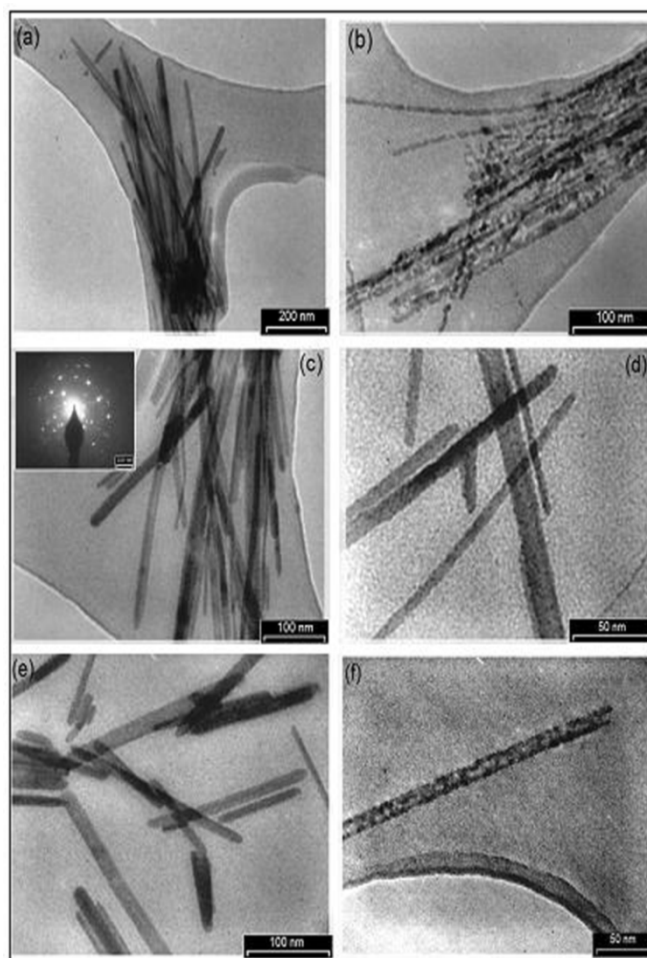

Fig. 7. TEM images of resulting cadmium oxide nanostructure with electron diffraction pattern in the inset (c).

Actually, the base of absorption is the excited state of electrons from the valance band to the conduction band, which can be used to determine value of *Eg*. The Tauc relation is given as follow [41]:

$$(\alpha h v)^n = B(h v - E_g) \qquad (1)$$

Where, hv is the photon energy, α is the absorption coefficient, B is a constant value and *Eg* is the direct optical band gap energy. The absorption coefficient (α) is estimated by the following relation:

$$\alpha = \frac{-1}{t}\ln T \qquad (2)$$

In this relation, T is the transmittance value and *t* is the thickness of the substance that places under UV-Vis irradiation.

After performing the whole experiments and determining the responses, these results are analyzed by calculating signal to noise ratio (S/N) for each experiment and analysis of variance (ANOVA). ANOVA represents error variance and the relative importance of the factors. In statistical analysis, three classes of the S/N ratio are considered: (1) the higher is the better (HB), (2) nominal is the best (NB), (3) the lower is the better (LB).

In this work, the LB type was chosen to obtain the most appropriate response. The S/N ratio is given as follows:

$$\frac{S}{N} = -10 Log \left(\frac{1}{n} \sum_{i=1}^{n} \frac{1}{Y_i^2} \right) \tag{3}$$

Where, n is the number of the repetitions under the same experimental conditions, Y is the result of measurement that in this study the band gap energy was selected as Y.

The response (Y) and signal to noise ratio(S/N) related to each experiment are presented in Table 3. The tests of 2 and 9 indicated the maximum and minimum values for Y; 2.19 and 1.83 eV and S/N ratio; 6.80 and 5.24, respectively. The mean of S/N ratio, $(M)_{Factor=I}^{Level=i}$, for each factor at a certain level is calculated by equation (4). The level with the minimum value is chosen as optimum level for the each factor.

$$M_{Factor=I}^{Level=i} = \frac{1}{n_{Ii}} \sum_{j=1}^{n_{Ii}} \left[\left(\frac{S}{N} \right)_{Factor=I}^{Level=i} \right]_j \tag{4}$$

In this equation, n_{Ii} is the number of appearances of the factor I in the level i.

The optimum conditions were predicated by considering the values of $(M)_I^j$ to synthesize the better structure with the most appropriate band gap energy (Table 4). In the theoretical estimation, considering the minimum state as the selected analysis, the average values of response and S/N ratio changed from 1.98 eV and 5.95 to 1.72 eV and 4.82, respectively.
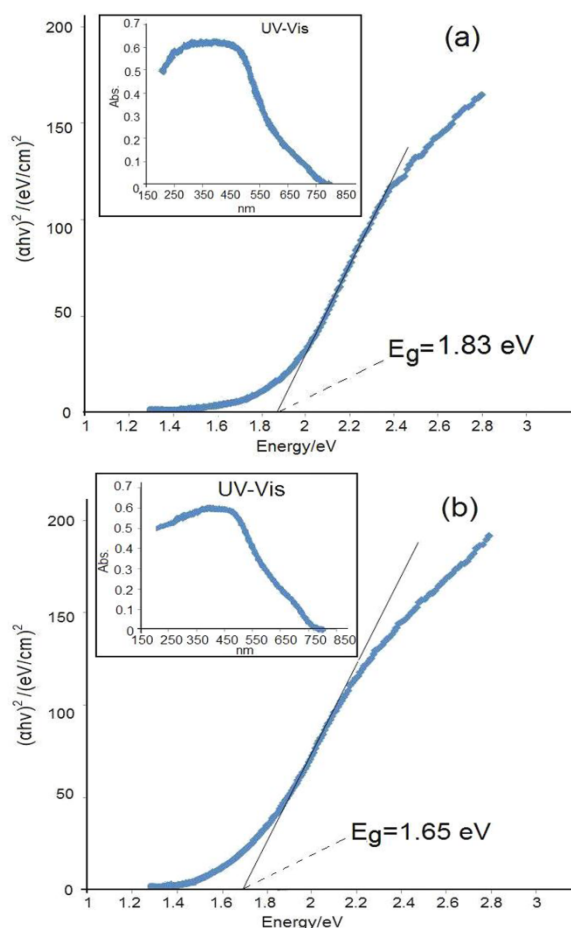

Fig. 8. The plot of (αhν)^2 *vs.* hν (eV) for determining direct band gap energy of the resulting CdO nanostructure with UV-Vis spectrum in the inset. (a) is the theoretical estimation and (b) is the obtained value from running the optimal experiment.

Table 4. Optimum conditions.

Factors	Teperature of calcining (˚C)	Duration of milling (min)	Duration of calcining (h)	M/L ratio (molar)
Predicated Optimum conditions	550	90	6	3:2

Table 5. Analysis variance (ANOVA) data.

Factors	DOF_F	Sum of Sqrs. (SS_F)	Variance (V_{Er})	Percent P_F (%)
Temprature of calcining	2	1.49	0.748	68.23
Duration of milling	2	0.03	0.015	1.38
Duration of calcining	2	0.38	0.194	17.72
M/L ratio	2	0.27	0.138	12.64

Table 6. Comparison the Test 9 and Optimal Test.

Test	Calcining temprature	Milling during	Calcining time	M/L	Y	S/N
9	550	90	4	3:2	1.83	5.24
Optimal	550	90	6	3:2	1.65	4.35

When the optimal conditions was run, the mentioned results practically altered to 1.65 eV and 4.35, which introduce the best performance of the prepared nanostructure.

Analysis of variance (ANOVA) is another technique at the statistical calculations, which is used to study the relative influence of factors and their interactions (Table 5). In this Table, P_F is the percentage contribution of each factor that obtains through the relation of 5:

$$P_F = \frac{SS_F - (DOF_F V_{Er})}{SS_T} \times 100 \qquad (5)$$

Where, DOF_F is the degree of freedom for each factor that is DOF_F = L-1 (L is the number of level for each factor). SS_T is the total sum of squares that is determined according to relation (6).

In this equation, m and n present the number of experiments and the number of the repetitions, respectively. $\overline{Y_T}$ is the total average value of the measured results that can be computed by equation (7).

$$SS_T = \sum_{J=1}^{m} \left(\sum_{i=1}^{n} Y_i^2 \right)_J - mn \left(\overline{Y_T} \right)^2 \qquad (6)$$

$$\overline{Y_T} = \frac{\sum_{j=1}^{m} \left(\sum_{i=1}^{n} Y_i \right)_J}{mn} \qquad (7)$$

Yi is the response of experiment that in this work, the band gap energy has been chosen as Yi. Meanwhile, SS_F is the factorial sum of squares, which was estimated using the following relation:

$$SS_F = \frac{mn}{L} \sum_{k=1}^{L} \left(\overline{Y_K^F} - \overline{Y_T} \right)^2 \qquad (8)$$

$\overline{Y_K^F}$ is the average value of the results for each factor measured at Kth level. V_{Er} is the error variance that was computed by relation (9).

$$V_{Er} = \frac{SS_T - \sum_{F=A}^{D} SS_F}{m(n-1)} \qquad (9)$$

With attention to the mentioned calculations in Table 5, temperature and duration of calcining were revealed with percentages of 68.23 and 17.72%, respectively, which have high influence on the response. It was found that the temperature of calcining is the most influence factor chosen in this study. Practically, this effect can be attributed to change the component size of the nanostructure due to calcination step.
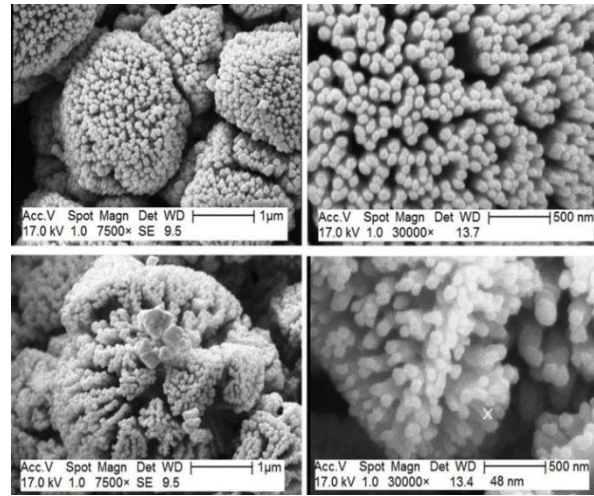

Fig. 9. SEM images of the optimal product.

Fig 9 shows the SEM images of the synthesized sample under the optimum conditions. Clearly, the decrease of component size of the cauliflower structure with uniform morphology is observed from 59 to 48 nm, which confirms the mentioned results. The participation curve and its pie chart of the main factors are indicated in Fig. 10. These findings show that all selected factors can be contributed to obtain the favorable conditions with different percentage. Also, it was observed that the proposed optimal experiment is comparable with the Test 9 from Table

2. These two tests are different at the factor of calcining time, which is led to improve response (Table 6).

Without further statistical calculations and easily obtained the promising conditions to synthesize cauliflower-like structure in nanoscale. In fact, the value of band gap energy was modified due to operate the proposed optimum conditions, which is the most important parameter in the photocatalytic activity of semiconductor materials.
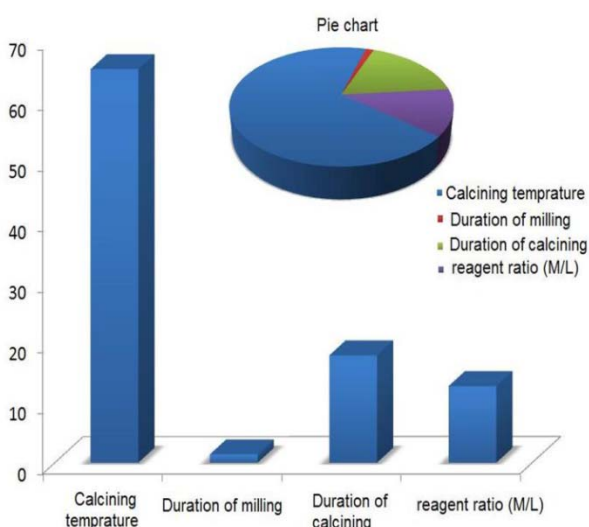

Fig. 10. The participation curve of the selected factors with its pie chart in inset.

4. Conclusion

In this study, the design of experiment was used to optimize the preparation of CdO nanostructure with the cauliflower-like morphology. This structure was synthesized via the mechanochemical reaction followed heating treatment. In order to reach this aim, nine experiments were designed using Taguchi method with considering four main factors and three levels for each factor. So the whole experiments were performed and the optimum conditions were predicted, which the results improved through running the optimum conditions. Moreover, the

uniform morphology with the smaller size of components obtained due to perform the optimal conditions. The percentage contribution of each factor to improve the response was studied and found the temperature and duration of calcination relative to other factors have the main role on the response. Obviously, mechanochemical reaction is a low- cost and useful method to synthesize the nanostructures in the laboratory and industrial scales and also, design of experiments (DOE) is an effective strategy to achieve in this goal as soon as possible.

References

[1] W. Dong, C. Zhu, Opt. Mater, 22 (2003) 227-233.

[2] R. Vinodkumar, K.J. Lethy, P.R. Arunkumar, R.R. Krishnan, N. Venugopalan Pillai, V.P. Mahadevan Pillai, R. Philip, Mater. Chem. Phys, 121 (2010) 406-413.

[3] T.J. Kuo, M.H. Huang, J. Phys. Chem, B 110 (2006) 13717-13721.

[4] Q. Chang, C. Chang, X. Zhang, H. Ye, G. Shi, W. Zhang, Y. Wang, X. Xin, Y. Song, Opt Commun, 274 (2007) 201-205.

[5] I. Akyuz, S. Kose, E. Ketenci, V. Bilgin, F. Atay, J. Alloys Compd, 509 (2011) 194.

[6] F. Atay, I. Akyuz, S. Kose, E. Ketenci, V. Bilgin, J Mater Sc: Mater Electron, 22 (2011) 492-498.

[7] S.A. Mayén-Hernández, G. Torres-Delgado, R. Castanedo-Pérez, J.G. Mendoza-Alvarez, O. Zelaya-Angel, Mater. Chem. Phys, 115 (2009) 530-535.

[8] A.A. Dakhel, Curr. Appl. Phys, 11(2011) 11-15.

[9] M.A. Grado-Caffaro, M. Grado-Caffaro, Phys. Lett. A, 372 (2008) 4858-4860.

[10] F. Yakuphanoglu, Appl. Surf. Sci, 257(2010)1413-1419.

[11] R.S. Mane, H.M. Pathan, C.D. Lokhande, S.H. Han, Sol. Energ, 80 (2006) 185-190.

[12] T.V.S. Sarma, S. Tao, Sensor Actuator B: Chem, 127 (2007) 471-479.

[13] A.S. Kamble, R.C. Pawar, J.Y. Patil, S.S. Suryavanshi, P.S. Patil, J. Alloys Compd, 509 (2011) 1035-1039.

[14] R.R. Salunkhe, C.D. Lokhande, Sensor. Actuator. B: Chem, 129 (2008) 345-351.

[15] R.K. Gupta, K. Ghosh, R. Patel, P.K. Kahol, J. Alloys Compd, 509 (2011)4146-4149.

[16] M.H. Kim, Y.U. Kwon, J. Phys. Chem. C, 113(2009) 17176-17182.

[17] X. Liu, C. Li, S. Han, J. Han, C. Zhou, Appl. Phys. Lett, 82(2003)1950-1952.

[18] F. Yakuphanoglu, M. Caglar, Y. Caglar, S. Ilican, J. Alloys Compd, 506(2010)188-193.

[19] R. Saravanan, H. Shankar, T. Prakash, V. Narayanan, A. Stephen, Mater. Chem. Phys, 125 (2011)277-280.

[20] G. Singh, I.P.S. Kapoor, R. Dubey, P Srivastava, Mater Sci Eng: B, 176 (2011)121- 126.

[21] J. Li, Y. Ni, J. Liu, J. Hong, J. Phys. Chem. Solid, 70(2009)1285-1289.

[22] A. Dakhel, A. Ali-Mohamed, J. Sol-Gel Sci. Technol, 55(2010)348-353.

[23] G. Choudhary, V. Raykar, S. Tiwari, A. Dashora, B.L. Ahuja, Phys. Status Solidi B, 248 (2011) 212-219.

[24] H.B. Lu, L. Liao, H. Li, Y. Tian, D.F. Wang, J.C. Li, Q. Fu, B.P. Zhu, Y. Wu, Mater. Lett, 62 (2008) 3928-3930.

[25] R.R. Salunkhe, D.S. Dhawale, U.M. Patil, C.D. Lokhande, Sensor Actuator B: Chem, 136 (2009) 39-44.

[26] T. Ghoshal, S. Kar, S.K. De Appl. Surf. Sci, 255(2009)8091-8097.

[27] A. Tadjarodi, M. Imani, Mater. Lett, 65 (2011) 1025-1027.

[28] M. Ramazani, A. Morsali, Ultrason. Sonochem, 18 (2011) 1160-1164.

[29] A. Askarinejad, A. Morsali, Chem. Eng. J, 150 (2009) 569-571.

[30] Z-x. Yang, W. Zhong, Y-x. Yin, X. Du, Y. Deng, C. Au, Y-w. Du, Nanoscale Res. Lett, 5 (2010) 961-965.

[31] M. Ghosh, C.N.R. Rao, Chem. Phys. Lett, 393 (2004) 493-497.

[32] H. Yang, G. Qiu, X. Zhang, A. Tang, W. Yang, J. Nanopart. Res, 6(2004)539-542.

[33] C. Suryanarayana, Progr. Mater. Sci, 46(2001)1-184.

[34] L.C. Damonte, M.A. Hernández-Fenollosa, B. Marí, J. Alloys Compd, 434-435 (2007).

[35] M. Mahmoodian, A.B. Arya, B. Pourabbas, Dental Mater, 24 (2008) 514-521.

[36] A. Coulibaly, B. Mutel, D. Ait-Kadi, Comput. Ind, 58 (2007) 567-577.

[37] G. Taguchi, R. Jugulum, The Mahalanobis-Taguchi strategy a pattern Technolog system, first ed., John Wiley & Sons, New York, 2002.

[38] M. Edrissi, R. Norouzbeigi, J. Nanopart. Res, 12 (2010) 1231-1238.

[39] S.C. Singh, R. Gopal, J. Phys. Chem. C 114 (2010) 9277-9289.

[40] S. Singh, R. Swarnkar, R. Gopal, J. Nanopart. Res, 11 (2009) 1831-1838.

[41] N. J. Tharayil, R. Raveendran, A. V. Varghese, P. G. Chithra, Indian J. Eng. Mater. Sci, 15 (2008) 489-496.